RSC Advances

ROYAL SOCIETY OF CHEMISTRY

www.rsc.org/advances

Cite this: DOI: 10.1039/c0xx00000x

www.rsc.org/xxxxxx

ARTICLE TYPE

Improved supercapacitor potential and antibacterial activity of bimetallic CNFs-Sn-ZrO_2 nanofibers: Fabrication and characterization

Young-Sang Jang[a], Touseef Amna[b], M. Shamshi Hassan[*, a], Ja-Ram Gu[c], Hyun-Chel Kim[d], Jong-Hui Kim[e], Sang-Ho Baik[e], Myung-Seob Khil[*, a]

Abstract

The objective of our study was to develop a new class of one-dimensional Sn-ZrO_2 nanocrystals decorated CNFs. The utilized CNFs-Sn-ZrO_2 composite was prepared by sol–gel electrospinning method using polyacrylonitrile, $ZrO(NO_3)_3.2H_2O$ and $SnCl_2.6H_2O$ as precursors. The physicochemical properties of the synthesized samples were characterized by X-ray diffractometer (XRD), energy dispersive X-ray analysis (EDX), electron probe microanalysis (EPMA) and scanning electron microscopy (SEM). The bimetallic CNFs–Sn-ZrO_2 composite possessed higher electrochemical capacitance and better stability than the monometallic and pristine samples as supercapacitor electrode materials. CNFs–Sn-ZrO_2 composite also exhibited admirable antibacterial activity. From the antimicrobial kinetic test results of *E. coli*; it was established that the composite (CNFs–Sn-ZrO_2) possess enhanced bactericidal activity than monometallic ones. The obtained high supercapacitance and bactericidal potential can be attributed due to the synergistic effect of Sn and ZrO_2 in the carbon nanofiberous matrix. These results suggest the applicability of fabricated nanofibers as electrode material for supercapacitors and as antibacterial agents for decontamination of water etc.

Introduction

Bimetallic materials composed of two different metals are of greater interest than the monometallic ones for the enhancement of the desired properties. This is because bimetallization can improve the properties of the original single metal and create a novel hybrid property, which may not be achieved by monometallic materials. One-dimensional (1D) carbon materials such as carbon nanofiber (CNFs), carbon nanotube and composites based on these nanostructures are attractive materials for electrochemical energy storage devices. They have been widely investigated because of their impressive uses in gas sensors [1], supercapacitors [2] and have also served as efficient platforms for building multifunctional composite materials [3]. The CNFs with their relatively lower manufacturing cost and excellent electrical conductivity are promising as effective fillers compared to CNTs [4, 5]. Recently, CNFs have attracted much attention because of their unusual structure and high specific surface areas and thus these ultrafine fibers can be used as high performance fillers or electrode in supercapacitors. Thus, the CNF based composites with desirable characteristics can be fabricated according to the requirements. It is anticipated that the composite of 1D carbon materials and zero-dimensional metal nanoparticles can contribute to supercapacitor efficiency. Zirconium oxide (ZrO_2) has several properties that make it a useful material. These properties include high density, hardness, electrical conductivity, wear resistance, high fracture toughness, low thermal conductivity, and relatively high dielectric constant. Because of its high refractive index and high oxygen-ion conduction, ZrO_2 has been applied as resistive heating elements, oxygen sensors, catalysts and fuel cells [6–9]. The use of totally stabilized zirconia in fuel-cell technology utilizes the good ionic conductivity of cubic zirconia at medium and high temperatures [10]. Similarly, tin metal has also been reported as one of the best electrode material as it has theoretical capacity of ~992 $mAhg^{-1}$ [11,12]. Tin Oxide has potential applications in various field, such as gas sensors [13], dye-sensitized solar cells [14], electrodes for lithium-ion batteries [15], catalysts [16], supercapacitors [17] and so forth. However, there is relatively lesser number of studies conducted on the colloidal dispersions of bimetallic nanoparticles embedded into polymer nanofibers for antibacterial purpose [18, 19]. Herein we fabricated CNFs-Sn-ZrO_2 composite by electrospinning method and applied as electrode material for supercapacitors and antibacterial agent. To our awareness there is no report on the fabrication and bactericidal effect of CNFs-Sn-ZrO_2 bimetallic nanofibers. Gram-negative bacterium *E. coli* is selected in the current study since it is a well studied model organism for antibacterial experiments. Nevertheless, earlier workers have incorporated silver ions into zirconium titanium phosphate for antibacterial activity [20]. In another study films of chitosan with both of zirconium and/or titanium were applied to cotton fabric to enhance the antibacterial effect of cotton fabrics [21]. Recently, Andr´e *et al* reported the bio-enabled growth of SnO_2 coatings on glass and their active role in the degradation of organic molecules upon direct exposure to sunlight and simultaneously strong biocidal activity [22]. In the present study fabricated bimetallic carbon nanofiberous composite showed improved antibacterial activity with better capacitance than pristine and monometallic carbon nanofibers. Thus the synthesized bimetallic nanofibers can serve as an efficient alternative for practical use in decontamination of water and as electrode material for suparcapacitors.

Experimental

Materials

Polyacrylonitrile (PAN, Mw=150,000) and $SnCl_2 \cdot 6H_2O$ (98%) was purchased from Sigma-Aldrich. Zirconium Nitrate Oxide Dihydrate was purchased from Kanto Chemical Company. *N, N*-dimethylformamide (DMF, 99.5 assays) was supplied from Showa Chemicals Ltd., Japan. Microbial strain *Escherichia coli* KCCM 13821 was purchased from the Korean Culture Centre of Microorganisms (KCCM). Tryptone soy broth (Torlak, Belgrade; BD Diagnostic, Becton, Dickinson & Co., USA) was used as a growth medium. All other chemicals and solvents used were of analytical grade extra pure chemicals purchased from Sigma.

Construction of CNFs-Sn-ZrO_2 composite by electrospinning

PAN solution (10 wt%) was prepared by dissolving PAN in DMF under magnetic stirring for 8 h at room temperature. Equal weight percent of $ZrO(NO_3)_3.2H_2O$ and $SnCl_2.6H_2O$ were added into the PAN solution, followed by vigorous stirring at room temperature to get homogeneous polymer solution. The resulting composite solution (PAN: $ZrO(NO_3)_3.2H_2O$ + $SnCl_2.6H_2O$; 1:1 w/w) was dispensed into a plastic syringe (working capacity-10 ml) with the help of micropipette. A copper pin connected to a high voltage generator was inserted in the solution as a positive terminal whereas a ground iron drum covered by a polyethylene sheet served as counter electrode. The solution was kept in the capillary by adjusting the inclination angle (~50°). A voltage of 15 kV was applied to this solution. The distance between the syringe tip and collector was fixed at 15 cm. The as-synthesized composite mat was stabilized in air at 280 °C for 1 h, and then calcined at 700 °C for 2 h with a ramping rate of 5 °C/min under N_2 atmospheres in a tubular furnace.

For comparison, CNF-ZrO_2 were also synthesized using $ZrO(NO_3)_3.2H_2O$ (10 wt%) as a precursor. Similarly pristine CNFs (without addition of any salt precursor) were also synthesized following exactly the same procedure as aforementioned.

Characterization

The XRD pattern of synthesized composite nanofibers was recorded on a Rigaku/Max-3A X-ray diffractometer with CuK radiation (λ=1.540 Å) and the operating voltage and current were maintained at 30 kV and 40 mA, respectively. To examine the surface morphology, the composite sample was uniformly sprayed on carbon tape and Pt coating was applied for approximately 10 s. The images were acquired at various magnifications using scanning electron microscopy (SEM, JEOL JSM6700, Japan). The elemental composition was identified by energy dispersive X-Ray analysis, whereas the distribution of elements was measured using electron probe microanalysis.

Electrochemical Characterization

Electrochemical measurement was carried out in a conventional three-electrode system using potentiostat (Digi-Ivy, USA). Glassy carbon electrode was used as a working electrode while Ag/AgCl electrode and a Pt wire were used as reference and counter electrode, respectively. For the working electrode (glassy carbon), different samples of synthesized nanofibers were prepared by dispersing 2 mg of each nanofiberous sample in a solution of 400 µl of isopropanol and 20 µl of nafion and were sonicated for 10 min. From this dispersion, 50 µl was placed on a glassy carbon electrode. The solvent was slowly evaporated by placing the electrode in an oven at 60 °C. Electrochemical measurements were conducted in 1M H_2SO_4 aqueous solution at room temperature. The specific capacitance (Cs) was calculated from CV curves calculated graphically by integrating the area under the CV curve using the following relation [23],

$$Cs = \int_{Va}^{Vc} IVdV \frac{1}{w \times \upsilon \times (Va - Vc)} \quad (1)$$

Where w is the mass of the electrode sample and υ is the sweep rate (Vs^{-1}).

Antibacterial assay

The antibacterial efficacy of pristine CNFs, CNFs-ZrO_2 and CNFs-Sn-ZrO_2 nanofibers were studied using the growth inhibition studies as described by Hassan and co-workers [24] with modifications against model organism *E. coli*. Briefly, inoculum was prepared from fresh overnight broth culture grown in Tryptone soy broth supplemented with yeast extract (0.6%) that were incubated at 37 °C. For antibacterial assay, the bacterial strains were first grown on solid nutrient medium and from the agar plates, fresh colonies were inoculated into the broth. Growth was monitored at regular intervals of time (3 hours) by UV-visible spectrophotometer (UV-2550, Shimadzu, Japan), till the optical density (OD) reached 0.1 at 600 nm (0.1 corresponded to a concentration of 10^8 CFU/ml). The pure suspension culture of bacterial density of 1×10^8 CFU/ml was used for seeding on the 100 ml of freshly prepared sterilized samples which was pre-exposed to pristine CNFs, CNFs-ZrO_2 and CNFs-Sn-ZrO_2 composite nanofibers solution. All the samples were incubated at 37 °C in a rotary shaker (rpm-150). Blank (culture broth) and inoculated controls (without nanocomposite material) were also kept. The growth rates were monitored by measuring the OD as described above at an interval of 3 h for 15 h.

Results and discussion

1. Characterization of pristine and composite nanofibers

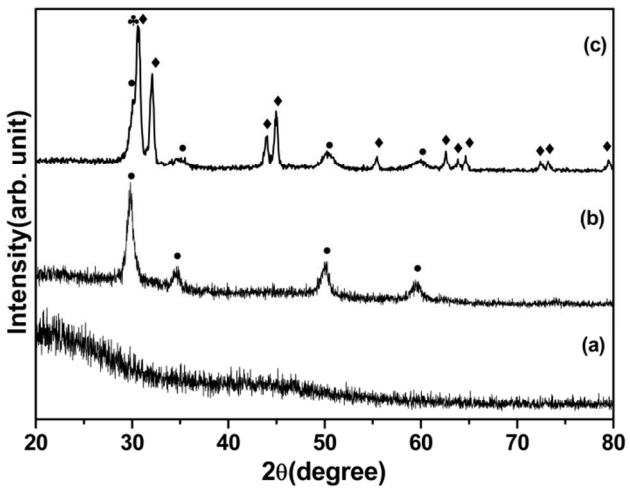

Fig. 1 XRD pattern of (**a**) CNFs (**b**) CNFs-ZrO_2 and (**c**) CNFs-Sn-ZrO_2 composite nanofibers calcined at 700 °C. Symbol (●) represents the ZrO_2, (♦) Sn and (♣) SnO peaks respectively.

Fig. 1 shows the XRD pattern of CNFs, CNFs-ZrO_2 and CNFs-Sn-ZrO_2 at 700 °C. The pristine CNFs showed no distinguish peaks because of the amorphous nature of the material (Fig.1a). For the ZrO_2 containing CNFs (Fig. 1b), four peaks at 30°, 35°, 50° and 60° were detected. They correspond to the (111), (200), (220) and (311) diffraction peaks of ZrO_2 (JCPDS No. 27-0997). This reveals the diffraction pattern of a cubic structure belonging to the space group Fm3m (225) with face centered lattice. The diffraction peaks of the CNFs-Sn-ZrO_2 composite were sharp and intense, indicating the highly crystalline character of the nanofibers (Fig. 1c). The peak in Fig. 1c confirms the presence of Sn tetragonal structure (JCPDS No. 89-4898) with cubic ZrO_2 phase in the composite. The characteristic overlapped diffraction peak at ~30° also indicates the presence of (101) plane of SnO minor phase (tetragonal, JCPDS No. 85-0712). So, from the XRD results it can be concluded that small amount of SnO phase is also present in the composite sample in addition to the Sn and ZrO_2 phases.

Figure 2 shows the SEM micrographs of the synthesized pristine CNFs, CNFs-ZrO_2, and CNFs-Sn-ZrO_2 composite, respectively at different magnifications after 700 °C annealing. The pristine

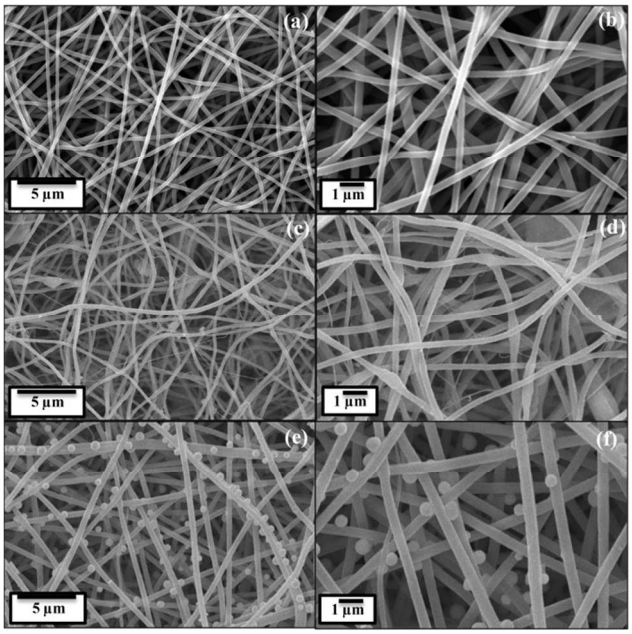

Fig. 2 SEM images of (**a, b**) CNFs (**c, d**) CNFs-ZrO_2 and (**e, f**) CNFs-Sn-ZrO_2 composite mat at low and high magnification.

CNFs are having a long fibrous morphology with smooth surfaces because of the amorphous nature of the material (Fig. 2a, b). The average diameter size of the fibers was found in the range of 300 ± 20 nm. Figure 2c, d shows the images of zirconia doped carbon nanofibers. A similar fibrous morphology was obtained except the fiber is thinner and the diameter ranged between 200 to 250 nm. After adding Zirconia precursor, $ZrNO_3.6H_2O$, in polyacrylonitrile solution, zirconium ions releases in solution which in turn increases the conductivity of the solution. The increase in the conductivity generally leads to decrease in the diameter of the fibers [25]. Conversely, prominent spherical crystals were seen in zirconia/tin composite nanofibers. These spherical crystals might be Sn nanoparticles having an average diameter of ~400 nm. The diameter size of the composite nanofibers was in the range of 400 to 500 nm (Fig. 2e, f). In case of CNFs-Sn-ZrO_2, the conductivity of composite is countered by the increase in viscosity in the solution, which leads to increase in fiber diameter.

Fig. 3 shows the Energy-dispersive X-ray spectroscopy (EDX) analysis of the CNFs-Sn-ZrO_2 composite. The peak corresponding to Sn, C, Zr and O are clearly identified. The elemental composition of the composite nanofibers was further confirmed by EPMA (Figure 4). The elemental mapping image clearly shows that Zr and Sn are uniformly dispersed on the surface of the CNFs.

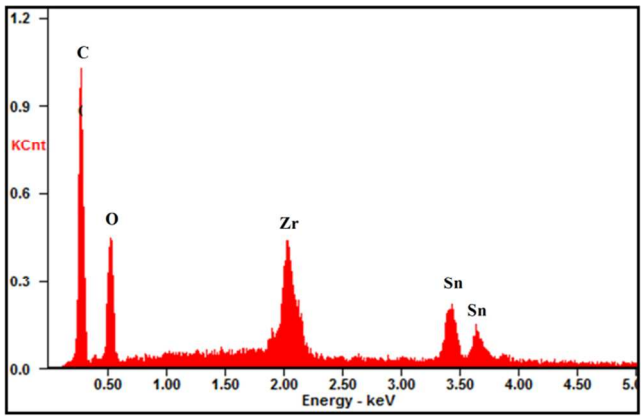

Fig. 3 EDX spectra of CNFs-Sn-ZrO_2 composite nanofibers.

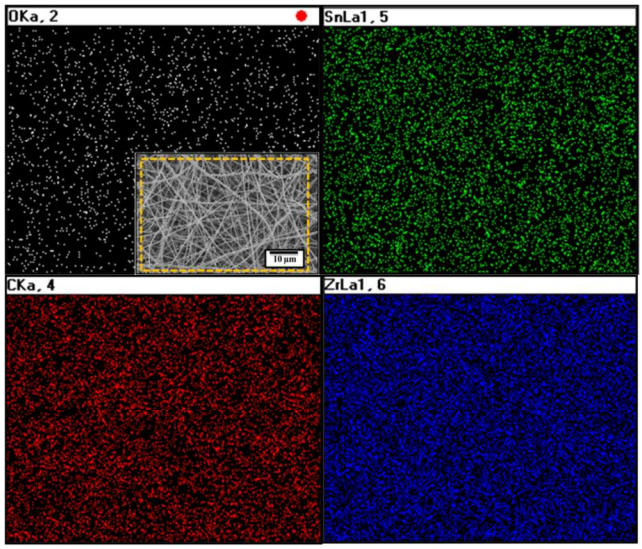

Fig. 4 Electron probe micro-analysis (EPMA) image of CNFs-Sn-ZrO_2 composite nanofibers. The red square in the *inset* represents the selected area.

2. Electrochemical properties

Fig. 5(a) shows the cyclic voltammograms (CV) of pristine CNFs, CNFs-ZrO_2, and CNFs-Sn-ZrO_2 composite nanofibers synthesized at 700 °C temperatures at a scan rate of 5 mV/s.

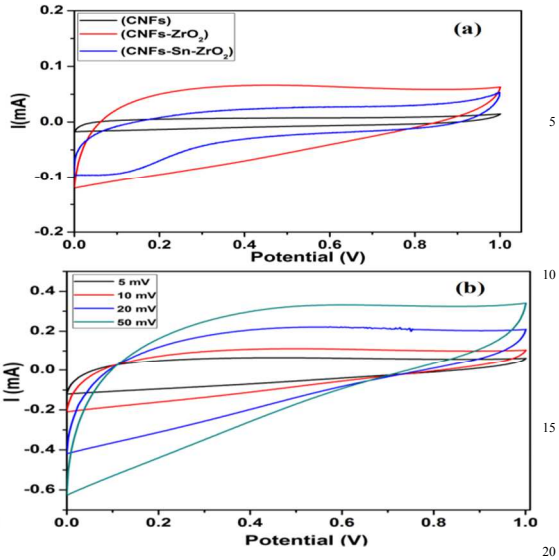

Fig. 5 (**a**) cyclic voltammograms of CNFs, CNFs-ZrO_2 and CNFs-Sn-ZrO_2 electrodes at a scanning rate of 5 mV/s and (**b**) CV of CNFs-Sn-ZrO_2 composite nanofiber at different scanning rates.

Compared with the CNFs and CNFs-ZrO_2, the nanocomposites CNFs-Sn-ZrO_2 exhibited higher current response and less estimated charge transfer resistance. It means the values of specific capacitance observed were higher for CNFs-Sn-ZrO_2 composite nanofibers (102.37 Fg^{-1}) than CNFs (14.34 Fg^{-1}) and CNFs-ZrO_2 (53.69 Fg^{-1}). This high capacitance value compared to the other samples may be due to the synergistic effect of Sn and ZrO_2 in carbon nanofiberous matrix, leading to an increase in the mobility of the charge carriers and enhancing the space charge capacitance. The rate performance of CNFs-Sn-ZrO_2 composite nanofibers was determined by studying the CV at different scanning rates as shown in Fig. 5(b). It can be seen that current under curve slowly increased with scan rate. This shows that the voltammetric current is directly proportional to the scan rates of CV, indicating an ideally capacitive behavior [26]. The specific capacitance of the CNFs-Sn-ZrO_2 composite nanofibers decreased from 102 to 42 F/g. This was mainly because the transfer rate of ions becomes slower with increasing scan rate which leads to either depletion or saturation of protons in the electrolytes inside the electrode during the redox process. This results in an increase in ionic resistivity which leads to a drop in the capacitance of the electrode [27]. The long-term chemical and electrochemical stability of the CNFs-Sn-ZrO_2 composite nanofibers was examined by CV at a scan rate of 10 mV/s over 100 cycles (Fig. 6).

The capacitance retention of CNFs-Sn-ZrO_2 composite still kept 94% of its initial capacitance. The better stability of CNFs-Sn-ZrO_2 came from the synergistic effect of Sn and ZrO_2 in carbon nanofibers matrix. So, this kind of composites can be considered as promising materials for the application of supercapacitors.

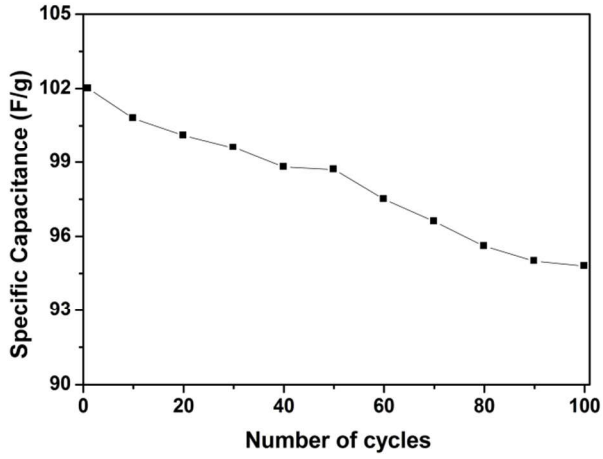

Fig. 6 specific capacitance variation of CNFs-Sn-ZrO_2 composite nanofibers as a function of cycle number.

3. Antibacterial activity

The Gram-negative bacterium *E. coli* is selected in the current study since it is a well studied model organism for antibacterial experiments. Antibacterial properties of electrospun CNFs, CNFs-ZrO_2 and CNFs-Sn-ZrO_2 composite nanofibers were tested using *E. coli*. For comparison, results for pristine CNFs nanofibers are also shown (Fig. 7a). CNFs, nanofibers without Sn/ZrO_2 compounds demonstrated a little antibacterial activity. Conversely, CNFs-ZrO_2 hybrid nanofibers showed noteworthy activity. Nevertheless, electrospun CNFs-Sn-ZrO_2 composite showed complete inhibition of *E. coli* indicating that nanofibers are endowed with excellent antibacterial properties due to the introduction of Sn and ZrO_2 on CNFs. In case of control samples logarithmic phase was found to be extended from 3-9 h or more (Fig. 7a). CNFs-Sn-ZrO_2 composite nanofibers have shown effective antibacterial activity against *E. coli.* Noticeable inhibition has been observed by CNFs-Sn-ZrO_2 composite during 3-15 h of incubation period.

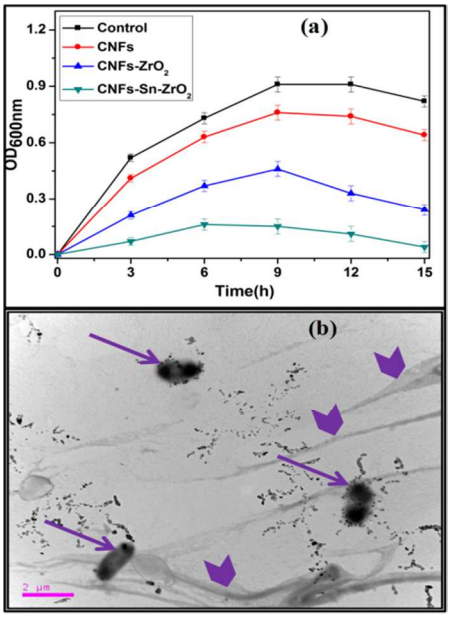

Fig. 7 (a) Growth kinetics of *E. Coli* cells exposed to different concentrations of CNFs, CNFs-ZrO_2 and CNFs-Sn-ZrO_2 composite mat. (**b**) Representative TEM image of exposed *Escherichia coli cells*.

Composite nanofibers with antibacterial potential have attracted huge interests in recent years. In fact, with the emergence and increase of microbial resistant to multiple antibiotics, many researchers/scientists have tried to develop new antibiotics. The bactericidal activity of semiconductor nanoparticles under visible light is very important in regards to its practical applications. The aim of this research is to compare the antibacterial activity of mono-metallic with bimetallic composite nanofibers using *E. coli* as a model organism. We selected ZrO and Sn as dopants in the present study. There are few reports on the antimicrobial properties of ZrO_2 and Sn nanocomposites against Gram negative and positive microorganisms. M. Gouda and N. Biswal *et al*., have reported the inhibitory effect of Zr composite on *E. coli* and *S. aureus* [20, 21] whereas Andr´e and co-workers have demonstrated antibacterial effect of SnO against *E. coli* in their study [22]. The exact mechanism is not fully clear in metal based polymeric materials. However, a plausible explanation for the microbial inhibition is that the nanoparticles are able to attach to the membrane of bacteria by electrostatic interaction and disrupt the integrity of the bacterial membrane [28]. It is reported that oxygen dissolved in the solution can generate superoxide anions (O^{-2}) by single-electron reduction, which does not require irradiation [29, 30]. The outstanding effect of the metal oxides, i.e. Zr oxide and Sn here could also reflect their ability to react with in cellular proteins, thereby inactivating and killing them more effectively than CNFs alone [31]. The synergistic effect of Zr oxide and Sn is also the reason for improved antibacterial action.

Conclusion

In the present investigation, we have been exploring the electrospinning process for the fabrication of CNFs-Sn-ZrO_2 composite nanofibers. The electrochemical studies proved that CNFs-Sn-ZrO_2 nanocomposite possessed a synergistic effect of Sn and ZrO_2 in carbon nanofiberous matrix, which showed higher capacitance and better stability than pristine and monometallic samples. The bimetallic CNFs-Sn-ZrO_2 composite nanofibers demonstrated excellent bactericidal effect against model organism *E. coli.* Conclusively new bimetallic CNFs-Sn-ZrO_2 composite nanofibers can be used as an efficient alternative for decontamination of water and as electrode material for supercapacitors.

Acknowledgement

This work was supported by the Industrial Strategic Technology Development Program, 10041994, funded by the Ministry of Knowledge Economy (MKE, Korea)

Notes and references

[a] *Department of organic materials and fiber Engineering, Chonbuk National University, Jeonju 561-756, Republic of Korea, E-mail:shamshi@jbnu.ac.kr, mskhil@jbnu.ac.kr, Fax:+82-63-270-2348, Tel:+82-63-270-4635.*

[b] *Department of Animal Sciences and Biotechnology, Chonbuk NationalUniversity, Jeonju, 561-756, Republic of Korea*

[c] *Nano Fusion Technology Research Group, Interdisciplinary Graduate School of Science and Technology, Faculty of Textile Science and Technology, Shinshu University, Ueda, Nagano, 386-0015, Japan.*

[d] *Department of Fashion Design & Textile Engineering, Chungwoon University, Hongseong-eup, Hongseong-gun, Chungnam, 350-701, Republic of Korea*

[e] *Department of Food Science and Human Nutrition and Research Institute of Human Ecology, Chonbuk National University, Jeonju 561-756, Republic of Korea*

[1] J. S. Lee, O. S. Kwon, S. J. Park, E. Y. Park, S. A. You, H. Yoon and J. Jang, *ACS Nano* 2011, **5**, 7992.

[2] J. Liu, J. Essner and J. Li, *Chem. Mater.* 2010, **22,** 5022.

[3] T. Wang and T. D. Lawrence, *ACS Appl. Mater. Interf.* 2012*,* **4**, 5079.

[4] M. J. Palmeri, K. W. Putz and L. C. Brinson, *ACS Nano,* 2010, **4**, 4256.

[5] C. Kim, Y. I. Jeong, B. T. N. Ngoc, K. S. Yang, M. Kojima, Y. A. Kim, M. Endo and J. W. Lee, *Small* 2007, **3,** 91.

[6] M.J. Mayo, J.R. Seidensticker, D.C. Hague and A.H. Carim, *Nanostruct. Mater*. 1999, **11,** 271.

[7] T. Chraska, A.H. King and C.C. Berndt, *Mater. Sci. Eng. A* 2000, **286**, 169-178.

[8] M. Gell, *Mater. Sci. Eng. A* 1995, **204,** 51.

[9] H. Gleiter, *Nanostruct. Mater*. 1992, **1**, 1.

[10] Y. Chen, S. Omar, A.K. Keshri, K. Balani, K. Babu, J.C. Nino, S. Seal and A. Agarwal, *Scripta Mater*. 2009, **60**, 1023.

[11] M. Winter and J. O. Besenhard, *Electrochim. Acta* 1999, **45**, 31.

[12] A. H. Whitehead, J. M. Elliott and J. R. Owen, J. Power Sources 1999, **81-82**, 33.

[13] F. Song, H. Su, J. Han, D. Zhang and Z. Chen, *Nanotechnol*. 2009, **20**, 495502.

[14] S. Gubbala, V. Chakrapani, V. Kumar, and M. K. Sunkara, *Adv. Funct. Mater*. 2008, **18**, 2411.

[15] Y. Idota, T. Kubota, A. Matsufuji, Y. Maekawa and T. Miyasaka, *Science* 1997 **276**, 1395.

[16] X. Cui, F. Cui, Q. He, L. Guo, M. Ruan and J. Shi, *Fuel* 2010, **89**, 372.

[17] R. K. Selvan, I. Perelshtein, N. Perkas and A. Gedanken, *J. Phys. Chem. C* 2008, **112**, 1825.

[18] H. R. Pant, D. R. Pandeya, K. T. Nam, W. I. Baek, S. T. Hong, H. Y. Kim, *J. Hazard. Mater*. 2011, **189** ,465.

[19] A. Yousef, N. A. M. Barakat, T. Amna, M. A. Abdelkareem, R. Afeesh, S. S. Al-Deyab and H. Y. Kim, *Macromol. Res*. 2012, **20**, 1.

[20] N. Biswal, S. Martha, U. Subudhi and K. Parida, *Ind. Eng. Chem. Res*. 2011, **50**, 9479.

[21] M. Gouda and S.M.A.S. Keshk, *Carbohydrate Polymers* 2010, **80,** 504.

[22] R. Andr´e, Filipe Natalio, M. N. Tahir, R. Berger and W. Tremel, *Nanoscale* 2013, **5**, 3447.

[23] S. K. Meher and G. R. Rao, *J. Phys. Chem. C* 2011, **115**, 15646.

[24] M. Shamshi Hassan, Touseef Amna, Faheem A. Sheikh, Salem S. Al-Deyab, K. E. Choi, I.H. Hwang and M. S. Khil, *Ceram. Int*. 2013, 39, 2503.

[25] R. Nayak, R. Padhye, I. L. Kyratzis, Y. B. Truong and L. Arnold, *Text. Res. J.* DOI: 10.1177/0040517512458347.

[26] C.C. Hu and T.W. Tsou, Electrochem. Comm. 2002, **4**, 105.

[27] T. P. Gujar, W.-Y.Kim, I. Puspitasari, K.-D. Jung and O.-S. Joolnt, *J. Electrochem. Sci*. 2007, **2**, 666.

[28] A. Thill, P. Zeyons, O. Spalla, F. Chauvat, J. Merose, M. Auffan and A.M. Flank, *Environ. Sci. Technol*. 2006, **40**, 6151.
[29] K. Hirota, M. Sugimoto, M. Kato, K. Tsukagoshi, T. Tanigawa and H. Sugimoto, Ceram. Int. 2010, **36**, 497.
[30] N. Talebian, S.M. Amininezhad and M. Doudi, J. Photochem. Photobiol. B Biol. 2013, **120**, 66.
[31] R. Purwar and M. Joshi, AATCC Review 2004, **4**, 22–25.

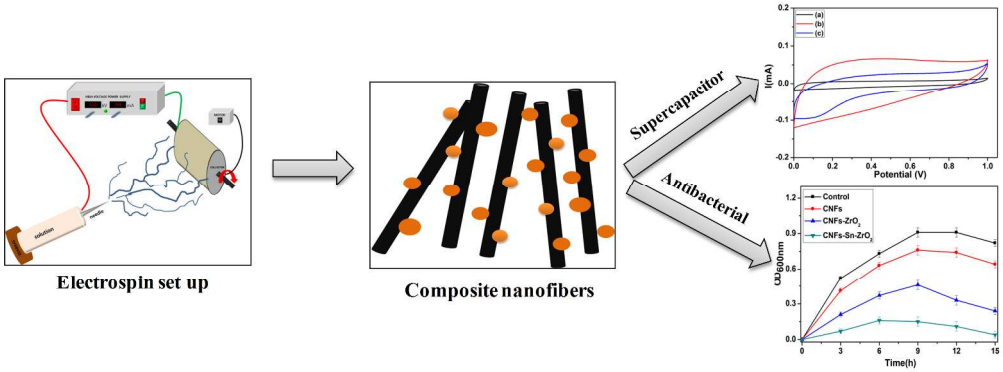

329x124mm (300 x 300 DPI)